INTRA-BEAM SCATTERING EFFECTS IN ELENA[*]

J. Resta-López, J. R. Hunt, C. P. Welsch,
Cockcroft Institute and The University of Liverpool, UK

Abstract

Intra-Beam Scattering (IBS) is one of the main limiting processes for the performance of low energy ion storage rings, such as the Extra Low ENergy Antiproton ring (ELENA) that is being constructed at CERN. IBS effects limit the achievable equilibrium 6D beam phase space volume during the cooling process, as well as the stored beam intensity. In this contribution we analyse the IBS effects on the beam dynamics of the ELENA ring in detail. Numerical simulations using the codes BETACOOL and MAD-X have been performed to compute the beam life time and the equilibrium phase space parameters with electron cooling in the presence of IBS.

INTRODUCTION

ELENA [1] is a small synchrotron equipped with an electron cooler, which is currently being constructed at CERN to further decelerate antiprotons from the Antiproton Decelerator (AD) [2] from 5.3 MeV to 100 keV kinetic energy with a beam population of $\sim 10^7$ cooled antiprotons. Electron cooling will be used to counteract the emittance and the momentum spread blow-up caused by the deceleration process. This will increase the intensity of antiprotons delivered to the antihydrogen experiments at the AD by one to two orders of magnitude.

The ELENA cycle is schematically shown in Fig. 1. There are two cooling plateaus: the first cooling plateau lasts approximately 8 s at 35 MeV/c momentum, and the second one is applied for 2 s at 13.7 MeV/c. In both cases the cooling is applied to a coasting beam. A third cooling at 13.7 MeV/c will be applied to bunched beams prior to extraction.
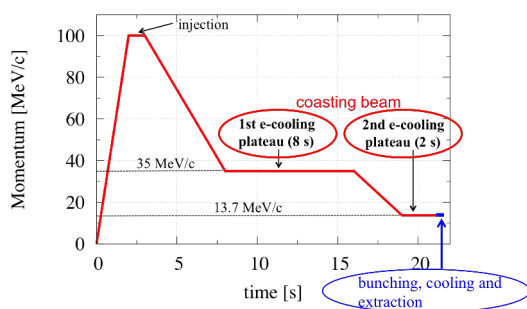

Figure 1: ELENA cycle.

A particular challenge for low energy ion storage rings, such as ELENA, is the question of achievable beam life time and stability. To address this question, we are investigating

the long-term beam dynamics in ELENA considering different effects limiting the achievable phase space volume obtained under electron cooling. Among these effects, IBS and rest gas scattering are important sources of beam heating.

For ELENA with the nominal vacuum pressure $P = 3 \times 10^{-12}$ Torr, it has been estimated that the effect of rest gas scattering would be practically negligible with respect to IBS [3, 4]. Therefore, in this paper we focus mainly on the study of the IBS effects.

IBS can be defined as a beam heating effect produced by multiple small-angle Coulomb scatterings of charged particles within the accelerator beam itself. It causes an exchange of energy between the transverse and longitudinal degree of freedom, thus leading to the growth of the beam phase space dimensions. The theory of IBS is extensively described in the literature, e.g. [5–8], and many of these IBS models are implemented in the simulation code BETACOOL [9,10]. This code allows us to calculate the evolution of beam distributions in the transverse and longitudinal phase space under the action of cooling and different scattering effects, and has been successfully benchmarked against experimental data, see e.g. [11].

IBS becomes stronger when the phase space volume of the beam is reduced by cooling, thus limiting the achievable final emittances, which are determined by an equilibrium state between IBS and cooling. In the next sections we investigate the beam evolution for the two ELENA cooling plateaus in the presence of IBS.

BEAM EVOLUTION

Beam dynamics simulations are performed using the code BETACOOL [9, 10], using the nominal beam parameters and electron cooling parameters adopted from [1,12] and the ELENA ring lattice with working point $Q_x \simeq 2.3$, $Q_y \simeq 1.3$ [13] in MAD-X format [14].

The simulations are based on a Monte-Carlo method (model beam algorithm of BETACOOL), with the following conditions: 1000 modelled macroparticles; electron cooling considering a cylindrical uniform electron beam distribution with transverse temperature $k_B T_{e\perp} = 0.01$ eV and longitudinal temperature $k_B T_{e\parallel} = 0.001$ eV; the cooling friction force is computed using the Parkhomchuk's model for a magnetised electron distribution [15]; rest gas and IBS effects are also included. For the IBS, the Martini model [7] is used. More details can be found in [4].

First Cooling Plateau

Let us consider first initial Gaussian distributions with relatively large rms transverse emittances and momentum

spread: $(\epsilon_x, \epsilon_y) = (8, 8)$ π mm·mrad, $\Delta p/p = 0.1\%$. Figure 2 shows the time evolution of these parameters during the first cooling plateau for 10 simulated random seeds. The corresponding beam profile distributions at different times of the cooling process are shown in Fig. 3. The beam distribution quickly deviates from a Gaussian profile and a very dense core appears.
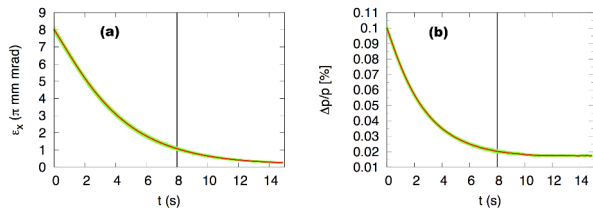

Figure 2: Evolution of the rms horizontal emittance (a) and momentum spread (b) over the first cooling plateau. The rms vertical emittance evolution is similar to (a).
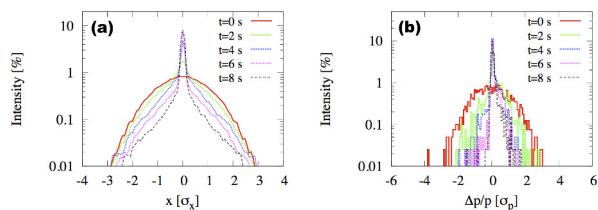

Figure 3: Horizontal (a) and momentum spread (b) distribution for different times during the first cooling.

Core-tail Development: For relatively large beam sizes at the beginning of the cooling, the beam distribution develops a very dense core and highly populated tails. This is due to the strength of the electron-antiproton friction force as a function of the relative velocity. Figure 4 shows the distribution of modelled antiprotons in the $(x, \Delta p/p)$ space at the beginning and at the end of the first cooling plateau. The parabolic momentum spread of the electrons due to space charge is also represented. Because of this space charge effect, antiprotons at large amplitudes experience a weaker friction force than those in the centre.

It is necessary to point out that in the case of cooling with large initial beam sizes, where the distribution quickly deviates from a Gaussian, the use of a standard IBS model, such as the Martini model, is probably underestimating the IBS effect for the core, thus leading to an overcooling of the core, as observed in Fig. 3. In the past, this was already noticed in [16]. Standard models of IBS are based on the growth of the rms beam parameters of Gaussian distributions. However, in the case of a non-Gaussian beam with a very dense core and large tails, it would be more correct to apply IBS induced kicks based on diffusion coefficients which are different for particles inside and outside of the core. Different IBS models for non-Gaussians distributions have been proposed in the literature [16–20], and implemented in the code BETACOOL [21].
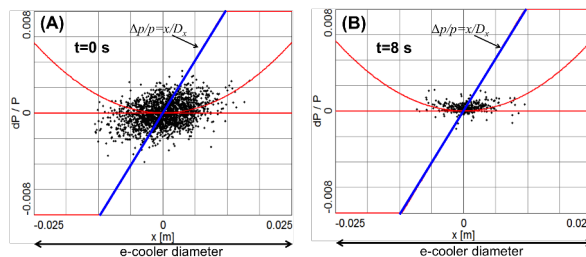

Figure 4: Distribution of an ensemble of 1000 modelled antiprotons in the cooler at $t = 0$ s (A) and at $t = 8$ s (B) for the first cooling plateau. The parabola represents the momentum spread of the electrons due to space charge charge. The straight blue line represents the dispersion line $\Delta p/p = x/D_x$ for the antiproton beam.

Applying an IBS core-tail model [16, 17], we have recalculated the time evolution of the ELENA beam distribution during cooling at 35 MeV/c, and compared it with the previous result where the IBS Martini model was applied (Fig. 5). The cooling of the core is smoother if an IBS core-tail model is applied and, probably, it describes more accurately the actual process.
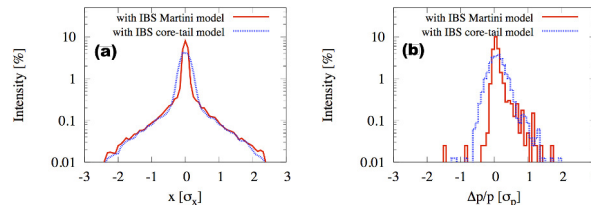

Figure 5: Horizontal (a) and momentum spread (b) distribution at $t = 8$ s for the first cooling plateau ($p = 35$ MeV/c), comparing the results using two different models of IBS: Martini model (solid red line) and a core-tail model (dotted blue line). The vertical distribution presents similar features to (a).

Second Cooling Plateau

For the second cooling plateau of a coasting antiproton beam at 13.7 MeV/c, Fig. 6 depicts the rms emittance and momentum spread as a function of time. For simplicity, in this case, we have adopted an initial Gaussian beam distribution with rms emittances $(\epsilon_x, \epsilon_y) = (2.8, 2.8)$ π mm·mrad and 0.05% momentum spread. These initial values take into account the adiabatic emittance increase by a factor $(\beta\gamma)_{35 \text{ MeV}/c}/(\beta\gamma)_{13.7 \text{ MeV}/c} \simeq 2.55$ because of the deceleration ramp from 35 MeV/c to 13.7 MeV/c. See Table 1 for a summary of the beam parameter values at the beginning and at the end of each cooling plateau.

Cooling of Bunched Beams

Before ejection, further cooling applied to bunched beams at 13.7 MeV/c momentum (for ~ 0.2–0.3 s) is planned to counteract IBS effects and reduce the phase space volume of

Table 1: Beam Parameters (rms Quantities) and Growth Rate Contributions from IBS ($1/\tau_x, 1/\tau_y, 1/\tau_p$)$_{\mathrm{IBS}}$ and E-cooling ($1/\tau_x, 1/\tau_y, 1/\tau_p$)$_{\mathrm{COOL}}$ before and after Cooling. The type of antiproton beam (coasting or bunched) and the cooling time are indicated. These results are the average over 10 modelled random seeds. For the growth rates, the negative sign indicates cooling.

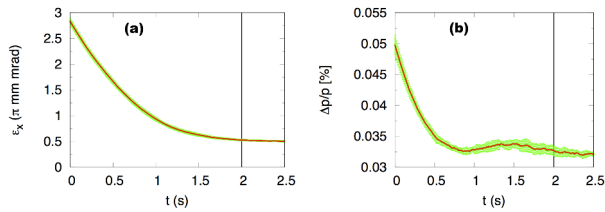| Cycle step	ϵ_x, ϵ_y [π mm·mrad]	$\Delta p/p$ [%]	$(1/\tau_x, 1/\tau_y, 1/\tau_p)_{\mathrm{IBS}}$ [s^{-1}]	$(1/\tau_x, 1/\tau_y, 1/\tau_p)_{\mathrm{COOL}}$ [s^{-1}]
Cooling at 35 MeV/c, coasting beam, 8 s				
Start	8.0, 8.0	0.1	$1.7 \times 10^{-4}, -2.5 \times 10^{-5}, 8.3 \times 10^{-4}$	-0.2, -0.2, -0.5
End	1.1, 1.1	0.02	0.02, -0.02, 0.7	-1.4, -1.4, -3.1
Cooling at 13.7 MeV/c, coasting beam, 2 s				
Start	2.8, 2.8	0.05	0.03, -0.009, 0.3	-1.1, -1.1, -1.9
End	0.52, 0.33	0.033	1.6, 1.8, 3.0	-2.5, -2.3, -4.5
Cooling at 13.7 MeV/c, bunched beam, 0.3 s				
Start	0.78, 0.49	0.049	2.6, 3.4, 0.7	-2.2, -2.0, -1.9
End	0.9, 0.55	0.043	1.7, 2.2, 1.7	-2.1, -2.0, -1.9

Figure 6: Evolution of the rms horizontal emittance (a) and momentum spread (b) over the second cooling plateau. The rms vertical emittance evolution is practically similar to (a).

bunches required by the experiments. Figure 7 compares the beam evolution between the cases with and without cooling for bunched beams. The cooling will keep transverse emittances < 1 π mm·mrad and momentum spread < 0.05%. In the bunching process we have assumed 50% emittance blow-up. Initial and final values of emittances, momentum spread and growth rates are written in Table 1.

OUTLOOK

IBS is one of the main heating processes limiting the achievable phase space volume during the beam cooling in low energy ion rings. In ELENA, it becomes significantly stronger at the second cooling plateau ($p = 13.7$ MeV/c) of the cycle and for cooling of bunched antiproton beams.

In this paper, BETACOOL simulations of the e-cooling process in ELENA are presented to describe the features of the beam evolution in the presence of IBS. The convenience of applying an IBS core-tail model is also discussed when large initial beam sizes are assumed at the beginning of the cooling process, as we have assumed here for the case of the cooling at 35 MeV/c.

Table 1 summarises the values of rms emittances and momentum spread as well as the IBS growth rates and cooling rates before and after the electron cooling.
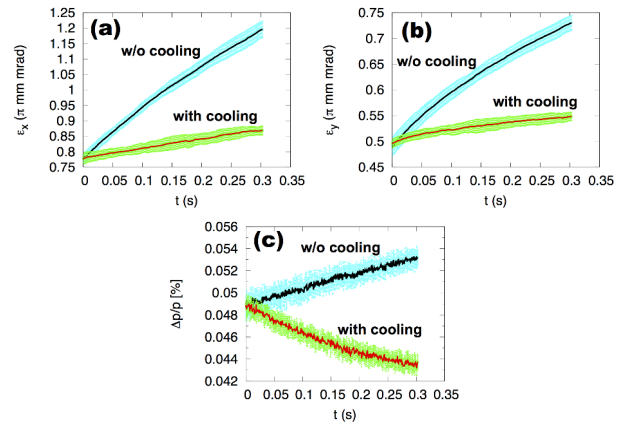

Figure 7: Evolution of the rms horizontal emittance (a), vertical emittance (b) and momentum spread (c) for bunched beams prior to extraction. The cases with and without cooling are compared.

It is also worth mentioning that for simplicity we have assumed initial Gaussian beam profiles. However, in practice, the distribution of the beam injected from the AD could have a dense core with significant non-Gaussian tails [22]. This characteristic will be taken into account in future studies.

ACKNOWLEDGMENTS

REFERENCES

[1] V. Chohan (editor), "Extra Low Energy Antiproton ring (ELENA) and its Transfer Lines, Design Report," CERN-2014-002 (2014).

[2] S. Maury (editor), "Design Study of the Antiproton Decelerator: AD," CERN/PS 96-43 (AR), 1996.

[3] C. Carli et al., "Review of Rest Gas Interaction at Very Low Energies Applied to the Extra Low Energy Antiproton Ring ELENA," Proc. of IPAC2014, TUPRI028, Dresden, Germany, 2014.

[4] J. Resta-Lopez at al., "Simulation studies of the beam cooling process in presence of heating effects in the Extra Low ENergy Antiproton ring (ELENA)," to be published in JINST.

[5] A. Piwinski, "Intra-Beam Scattering," Proc. of the 9th International Conference on High Energy Accelerators, Stanford, CA, 1974, p. 405.

[6] J. Bjorken, S. Mtingwa, "Intrabeam Scattering," Part. Accel. **13**, 115 (1983).

[7] M. Martini, "Intrabeam Scattering in the ACOL-AA Machines," CERN-PS-AA-84-9, 1984.

[8] A. Piwinski, "Intra-Beam Scattering," CERN Report 92-01 (1992), p. 226.

[9] A. Sidorin, Nucl. Instrum. Meth. A **558** (2006) 325.

[10] http://betacool.jinr.ru

[11] A. I. Papash et al., Phys. Rev. ST-AB **16** (2013) 060101.

[12] G. Tranquile et al., "The ELENA Electron Cooler: Parameter Choice and Expected Performance," Proc. of COOL2013, WEPPO16, Murren, CH, 2013.

[13] P. Belochitskii, "ELENA Project Status," Proc. of COOL2013, THPMIHA02, Murren, CH, 2013.

[14] http://mad.web.cern.ch/mad/

[15] V. V. Parkhomchuk, Nucl. Instrum. Meth. A **441** (2000) 9.

[16] A. V. Fedotov, "IBS for Ion Distribution Under Electron Cooling," Proc. of PAC05, Knoxville, Tennessee, USA, 2005.

[17] A. V. Fedotov, A. O. Sidorin, A. Smirnov, "IBS for Non-Gaussian Distributions," BNL-94081-2010-CP (2010).

[18] A. Burov, "Electron Cooling against IBS for High Energy Colliders," FERMILAB-TM-2213 (2003).

[19] G. Parzen, BNL Tech. Note C-AD/AP/150 (2004).

[20] P. Zenkevich, O. Boine-Frankenheim, A. Bolshakov, Nucl. Instrum. Meth. A **561** (2006) 284.

[21] BNL BETACOOL report, Dec. 2007: http://betacool.jinr.ru/reports

[22] C. Carli, private communication.